CrystEngComm

ARTICLE

Received 00th January 20xx,

Accepted 00th January 20xx

DOI: 10.1039/x0xx00000x

www.rsc.org/crystengcomm

Anodic dissolution growth of metal-organic framework HKUST-1 monitored via *in situ* electrochemical atomic force microscopy

Stephen D. Worrall,*[a] Mark A. Bissett,[a] Martin P. Attfield *[b,c] and Robert A. W. Dryfe *[c]

In situ electrochemical atomic force microscopy (ec-AFM) is utilised for the first time to probe the initial stages of metal-organic framework (MOF) coating growth *via* anodic dissolution. Using the example of the Cu MOF HKUST-1, real time surface analysis is obtained that supports and verifies many of the reaction steps in a previously proposed mechanism for this type of coating growth. No evidence is observed however for the presence or formation of Cu_2O, which has previously been suggested to be both key for the formation of the coating and a potential explanation for the anomalously high adhesion strength of coatings obtained via this methodology. Supporting *in situ* electrochemical Raman spectroscopy also fails to detect the presence of any significant amount of Cu_2O before or during the coating's growth process.

Introduction

Metal-organic frameworks (MOFs) are a group of nanoporous, crystalline materials that possess exceptionally high porosities and specific surface areas.[1] Built up from metal ions, or metal-containing inorganic clusters, bound to each other *via* multivalent, heteroatom containing organic molecules; MOFs have been investigated as candidate materials for a huge range of applications.[2-7] MOFs are traditionally obtained as powders but for many of these potential applications it is desirable or even necessary to obtain the MOF as a coating. Whilst post-synthesis processing of MOF powders into coatings is possible it is often difficult,[8] and as a result a wide range of techniques to grow MOF coatings directly onto substrates have been developed.[9-14] Electrochemical techniques have proved popular[15, 16] with the anodic dissolution technique, first demonstrated by Ameloot *et al*[17] further developed via a BASF patent[18] for the mass production of MOFs via electrochemistry, utilised to produce the greatest variety of different MOFs as coatings.

Despite the prevalent use of this technique it is only recently that attempts have been made to gain a deeper mechanistic understanding of this process.[19, 20] As the first MOF grown *via* the anodic dissolution method the Cu MOF HKUST-1, composed of Cu^{2+} cations and 1,3,5-benzenetricarboxylic acid (BTC) ligands in a paddle wheel configuration (see Fig. 1), has been used for these studies.[21]

Campagnol *et al*[19] proposed a detailed mechanism for almost the entire growth process consisting of four steps; "initial nucleation", "island growth", "intergrowth" and "detachment". Each step of the proposed mechanism is well supported, if only through *ex situ* analysis. However, the mechanism by which "initial nucleation" of MOF crystals on the electrode occurs remains unclear as it was not observed directly in real time. Indeed, there is some debate as to whether "initial nucleation" of the MOF occurs on metal oxides formed at the surface of the anode during anodic dissolution rather than just the bare metal anode surface. Schafer *et al*[20] identified that the presence and/or formation of Cu_2O on the Cu anode surface was key to form a MOF HKUST-1 coating in the absence of water. They were able to show that if the initial presence and subsequent growth of Cu_2O was minimised then so was the MOF coating growth.[20] They suggested that the Cu_2O on the electrode surface undergoes a

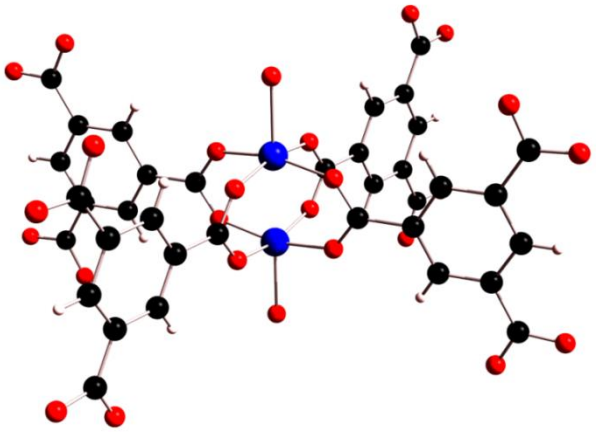

Fig. 1 Paddle wheel structure adopted by Cu^{2+} cations and BTC anions within the HKUST-1 framework. Copper is represented in blue, oxygen in red, carbon in black and hydrogen in white.

[a] School of Materials, The University of Manchester, Oxford Road, Manchester, M13 9PL, UK. E-mail: stephen.worrall@manchester.ac.uk
[b] Centre for Nanoporous Materials, School of Chemistry, The University of Manchester, Oxford Road, Manchester, M13 9PL, UK. E-mail: m.attfield@manchester.ac.uk
[c] School of Chemistry, The University of Manchester, Oxford Road, Manchester, M13 9PL, UK. E-mail: robert.dryfe@manchester.ac.uk

conversion to HKUST-1. Schafer *et al*[22] also showed that in the presence of small quantities of water no surface Cu_2O could be detected during anodic dissolution of a copper electrode to form HKUST-1. Similarly, Stassen *et al*[23] proposed the involvement of zirconium oxide films in the anodic deposition of UiO-66.[24] A detailed *in situ* study of the electrode/solution interface, prior to and during the initial stages of coating growth would help to further investigate the validity of these proposed mechanisms.

In situ atomic force microscopy (AFM) is a well-established technique for monitoring the nucleation and growth of MOFs;[25-27] the growth of HKUST-1 has been studied in particular.[28] However to the authors knowledge in situ electrochemical AFM (ec-AFM), where the substrate being analysed by AFM is the working electrode in the electrochemical set up, has not been applied to monitor the electrochemical nucleation and growth of MOFs. The technique has however been demonstrated to work for monitoring in real time the growth of other materials on electrode surfaces.[29] Here we demonstrate for the first time the use of in situ ec-AFM to monitor the nucleation and growth of the MOF coating during the anodic dissolution method. The results support much of the mechanism proposed by Campagnol *et al*[19] but cast doubt on the role of Cu_2O as a key intermediate in the coating growth process, with supporting *in situ* electrochemical Raman spectrometry measurements also providing no evidence for the presence or formation of Cu_2O during the growth process.

Experimental

Materials

The following materials were used as received for the experiments described subsequently. BTC (95%) was obtained from Aldrich. Cu sheet (OHFC Alloy 101 0.81 mm thick) was obtained from Alfa Aesar. Ultra-pure water (18.2 MΩ cm resistivity) was obtained from a Milli-Q Millipore Direct 8 purification unit. Ethanol (≥99.8%) and methyltributylammonium methyl sulphate (MTBAMS) (≥95%) were obtained from Sigma Aldrich.

In situ electrochemical atomic force microscopy

In situ ec-AFM of the electrode surface during the growth of a HKUST-1 coating was performed using a Multimode 8 Atomic Force Microscope (Bruker, USA), operating in PeakForce QNM mode with ScanAssyst activated. MPP-21100-10 Sb (n) doped Si cantilevers were used, with the tips mounted inside of an MMTMEC electrochemistry tapping fluid cell. A small, machined piece of Cu sheet was used as the working electrode (the electrode being imaged by the AFM) and Pt wire was utilised as the counter and pseudo-reference electrodes. The AFM was aligned and then the desired potential was chosen on the UNIVECPOT bipotentiostat, but no potential was yet applied. The electrolyte solution (48 mM BTC, 64 mM MTBAMS in 75:25 vol% ethanol:water) was then syringed into the fluid cell. The cell was then immediately set on, applying the set potential, and the cantilever was engaged with the surface to allow imaging to commence.

In situ electrochemical Raman spectroscopy

Confocal Raman spectroscopy of the anode surface was performed using a Renishaw inVia microscope during the growth of a HKUST-1 coating, as described below. Two Cu electrodes of equal geometrical area were immersed into the electrolyte solution (48 mM BTC, 64 mM MTBAMS in 75:25 vol% ethanol:water) ~ 2 cm apart and connected as anode and cathode to a PGSTAT302N Potentiostat (Metrohm Autolab B. V., The Netherlands). A 633 nm (1.96 eV) laser excitation at a power of 10 mW was used with a 50 x objective and a grating of 600 l mm^{-1} to achieve a spectral resolution of ca. 2 cm^{-1}. The laser was focussed onto the anode surface before the HKUST-1 growth was commenced. Chronoamperometry was then performed by applying a fixed potential of 2.5 V between the anode and cathode and to monitor the HKUST-1 growth on the anode surface. 10 s accumulations were taken every 10 s, or 1 s accumulations every 1 s, for up to 5 minutes.

Results and discussion

In situ electrochemical atomic force microscopy

A range of potentials vs Pt were applied to the Cu substrate with the aim of identifying the least anodic potential that could cause the HKUST-1 coating growth to occur. Identifying this potential is desirable as the MOF formation process will be slowed, which will facilitate the AFM imaging of the nucleation and growth of the coating. Extensive testing identified -225 mV vs Pt as the least anodic applied potential that would still result in the growth of the HKUST-1 coating. Interestingly at even less anodic potentials whilst dissolution of the Cu substrate was still observed to occur, even after over an hour of imaging no HKUST-1 coating growth was seen. This supports the first step in the theory posited by Campagnol *et al*[19] of "initial nucleation". This states that a "critical concentration" of Cu^{2+} cations at the anode surface is required to initiate coating growth; thus explaining why they observed the mass of the anode to first decrease, due to dissolution of the Cu, before it began to increase again, due to formation of the HKUST-1 coating. The length of time that the anode loses mass for is inversely proportional to the applied potential, as the more anodic the applied potential the higher the rate of production of Cu^{2+} and the faster the "critical concentration" will be reached.[19] However as the produced Cu^{2+} is also moving away from the anode surface, both via diffusion and migration in the electric field, if the rate of Cu^{2+} production is too low then it is possible that the "critical concentration" will never be reached. This argument would explain why at -225 mV vs Pt HKUST-1 coating growth was observed to occur in our system whilst at the less anodic potential of -250 mV no coating growth was observed despite clear evidence of Cu dissolution as seen in Fig. 2. It should also be noted that as we

have here intentionally slowed the reaction down the time before HKUST-1 growth starts, during which only dissolution of the Cu surface is observed, is significantly longer than that observed by Campagnol *et al*.[19]

At -225 mV vs Pt the period during which only dissolution of the Cu surface was observed lasted for approximately 19 minutes and was split in two stages as shown in Fig. 3. The first stage lasted approximately 12 minutes during which only very slow dissolution is observed (first five frames in Fig. 3). The second stage lasted a further 7 minutes during which the rate of Cu dissolution appears to increase (the next four frames in Fig. 3) to around 22 nm min^{-1}, measured by observing a feature receding laterally on the Cu surface as seen in Fig. 4. During this time the solution begins to turn a light blue colour and starts to cloud due to crystal formation in solution but no HKUST-1 crystals are observed on the electrode surface. It is also worth noting that this fairly rapid rate of dissolution of the Cu electrode, prior to any surface nucleation of HKUST-1 being observed, is seemingly incompatible with Cu_2O on the electrode surface playing a role in the formation of a HKUST-1 coating as proposed by Schafer *et al*.[20] Any Cu_2O present on the electrode surface prior to the application of a potential, or any formed as a result of it, would most likely be lost from the surface with the dissolving Cu. The potential role of Cu_2O is discussed further in the next section focussed on *in situ* electrochemical Raman spectroscopy.

In the image taken after 21 minutes the first crystal is observed to have nucleated at a defect on the rough electrode surface. This crystal is observed to grow in the subsequent images taken after 24, 26, 28 and 31 minutes (the next five frames in Fig. 3 and Fig. 5). At the same time many other crystals are also observed to nucleate near the original crystal. This observation of a sudden increase in the number of crystals nucleating in close proximity to an existing crystal supports the theory posited by Campagnol *et al*[19] of "island growth". Island growth is hypothesised to occur due to a local increase in current density around existing crystals on the Cu surface as compared to the bare electrode.[19] This local increase in current density results in a greater local Cu^{2+} concentration in the electrode/solution interface close to existing crystals, leading to an increase in the rate of new crystal nucleation in close proximity to existing crystals on the surface.

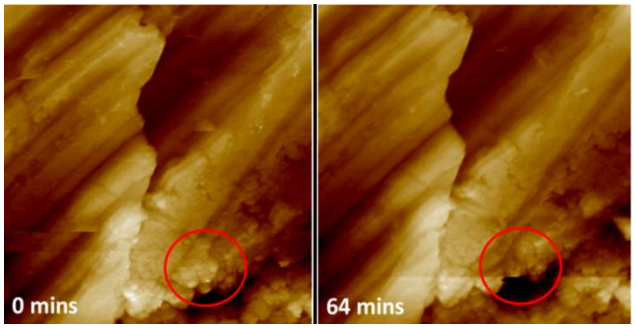

Fig. 2 Height AFM images taken during 64 minutes of the slow dissolution of a Cu electrode at an applied potential of -250 mV vs Pt. The red circle highlights one area of dissolution of the Cu anode. Each image is 10 x 10 µm.

In the final 5 minutes of the experiment the quality of the images noticeably deteriorates due to the combination of the high scan speed necessary for an *in situ* experiment and the increasingly rapid rate of change of the surface morphology of the electrode (the last two frames in Fig. 3). The HKUST-1 crystal whose growth was followed between 21 and 31 minutes is observed to have detached and numerous other crystals appear to be nucleating and detaching at a rapid rate. Whilst the theory of Campagnol *et al*[19] includes a final detachment stage, caused by the undercutting of the underlying Cu electrode to which the HKUST-1 is attached, this is not believed to occur until a much more extensive and inter-grown HKUST-1 coating has been obtained and therefore cannot explain the behaviour observed here. We hypothesise that this behaviour is caused by the rapid movement of the cantilever agitating the solution in the proximity of the area of the electrode being imaged. This agitation will disrupt the normal growth process with the forces generated sufficient to dislodge HKUST-1 crystals in the early stages of growth from the electrode surface. The probability of a crystal being dislodged would increase, at least initially, with the crystal size due to the longer contact time between the AFM tip and the crystal as it begins to increase in size.

The experiment was stopped after 36 minutes as the solution clouding, due to HKUST-1 crystal growth in solution, mentioned earlier became so severe that it sufficiently disrupted the laser path back from the cantilever to the detector so as to make further imaging of the surface impossible. It is worth noting that even during the relatively short period, of intentionally slow growth observed during this experiment that significant pitting and erosion of the electrode surface is observed. It is possible that the reason fully grown coatings of MOFs obtained via the anodic dissolution method have been observed to be strongly adhered to the underlying electrode surface[23] is due to this pitting. The significantly roughened electrode surface that results from the erosion will lead to a significantly greater contact area between the fully grown MOF coating and the underlying electrode surface than simply the geometric area. This greater contact area could result in a significantly increased extent of interaction between the fully grown MOF coating and the underlying electrode and lead to the increased strength of adhesion observed.

In situ electrochemical Raman spectroscopy

As the results of the *in situ* ec-AFM investigations do not appear to support the role of Cu_2O in the formation of the HKUST-1 coating as proposed by Schafer *et al*[20], *in situ* electrochemical Raman spectroscopy was utilised in order to see whether Cu_2O could be detected in the early stages of coating growth.

Initially a HKUST-1 powder sample was analysed using *ex situ* Raman spectroscopy in order to identify the most suitable peak to be used to track the growth of HKUST-1 at the electrode surface during subsequent *in situ* Raman spectroscopy measurements. The peak marked with an asterisk at approximately 1000 cm^{-1} in Fig. 6 was chosen as it

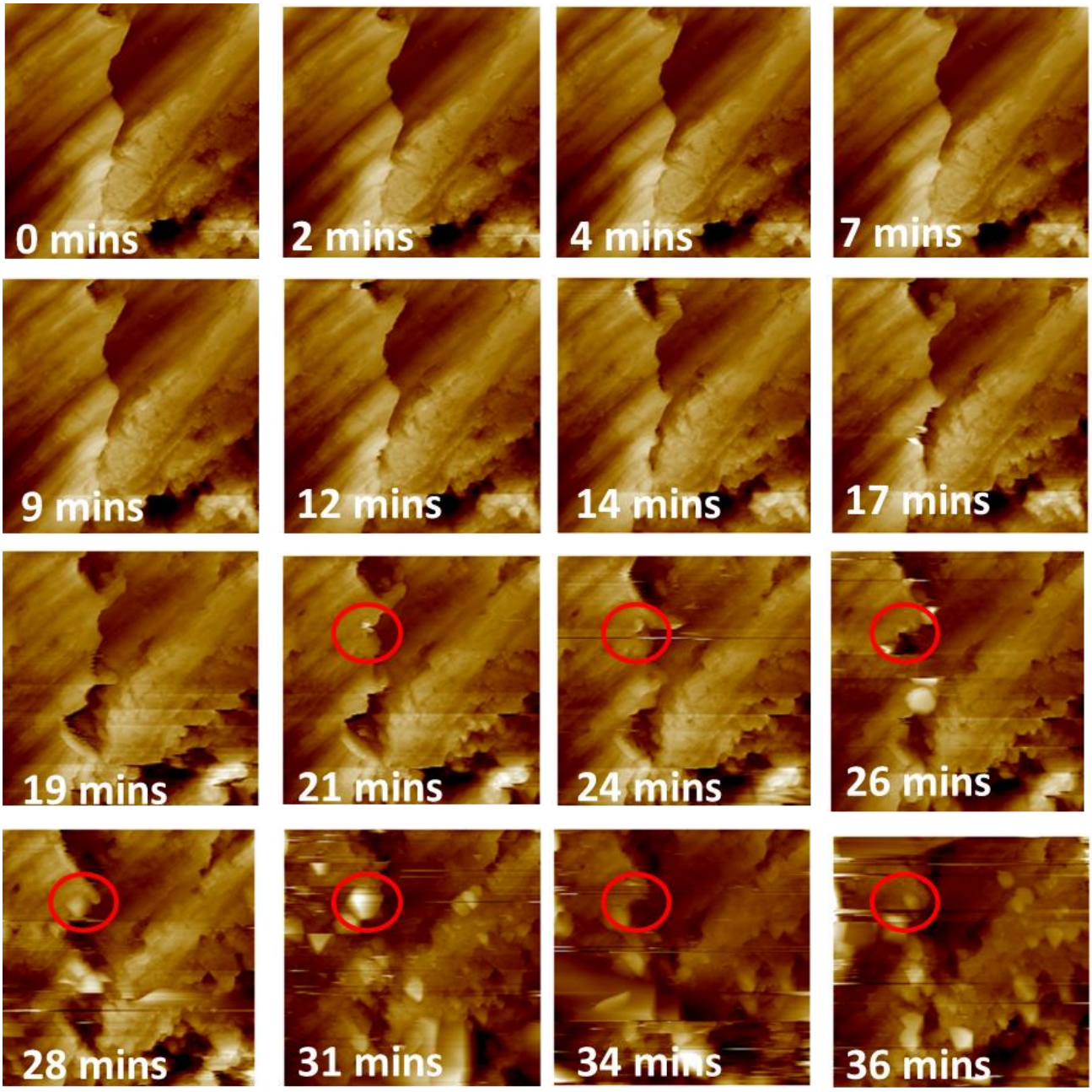

Fig. 3 Height AFM images taken during 64 minutes of the electrochemical growth of a HKUST-1 coating at an applied potential of -225 mV vs Pt. The red circle highlights the nucleation, growth and detachment of one HKUST-1 crystal. Each image was 10 x 10 µm.

exhibited a strong signal and did not overlap with any peaks from the electrolyte system.

In situ Raman spectroscopy was performed with 1 s accumulations every 1 s for 2 minutes and the spectra are presented in Fig. 7. For clarity the intensity of the major HKUST-1 peak at approximately 1000 cm^{-1}, relative to the peak intensity of a background electrolyte solution peak at 2930 cm^{-1}, as a function of time is also plotted in Fig. 7.

The HKUST-1 signal can be observed to begin to increase after about 10 s from the experiment start. This observation of growth of HKUST-1 after approximately 10 s of starting the process corroborates the work by Campagnol *et al*[19] who, using a quartz crystal microbalance, observed only a few seconds at the start of growth in which the anode loses mass, due to the dissolution of the anode, before mass begins to increase as a result of HKUST-1 deposition. It is worth pointing out here that the applied voltage in this *in situ* electrochemical Raman spectroscopy experiment was the same as that utilised by Campagnol *et al*[19] which explains why the delay between application of the potential and the start of HKUST-1 growth is much shorter than in the *in situ* ec-AFM experiments discussed above.

The Raman spectra of Cu_2O are characterised primarily by a pair of peaks at approximately 520 cm^{-1} and 620 cm^{-1} [30], neither of which is observed throughout the experiment. This observation suggests that either Cu_2O is present only at a very

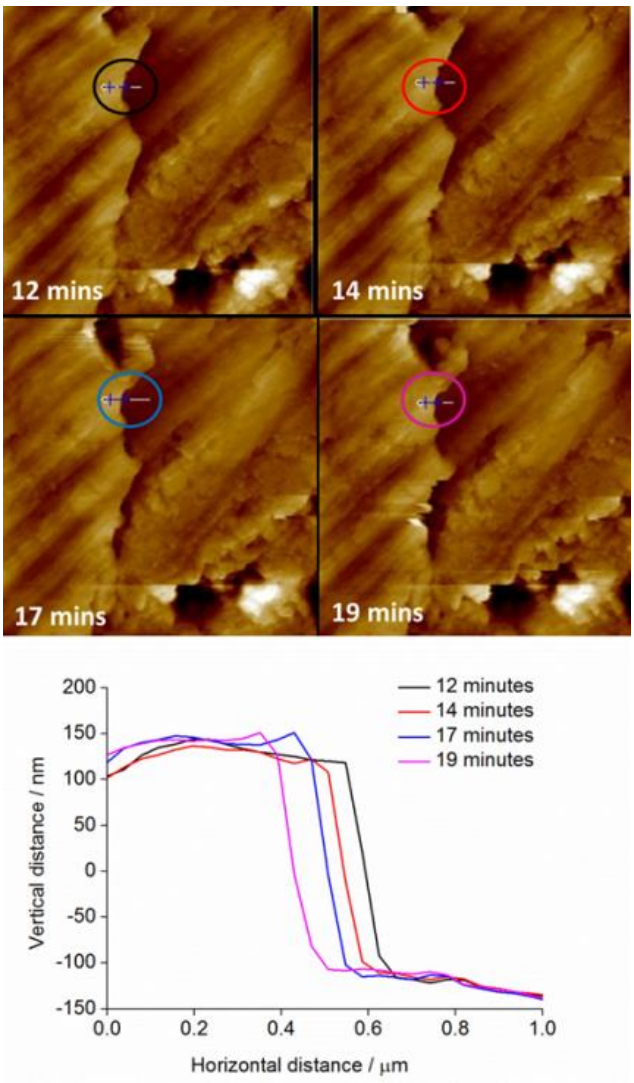

Fig. 4 Height AFM images, 10 x 10 μm, taken during electrochemical growth of a HKUST-1 coating with cross sections (top) plotted (bottom) to show the dissolution of the Cu electrode surface prior to HKUST-1 growth.

low concentration at any given time on the electrode surface, below the detection limit, or potentially that it is not in fact the growth intermediate. Whilst the Raman measurements here are not solely sensitive to surface species, as evidenced by the strong signals from the ethanol based solution in Fig. 7, the fact that both this study and the previous *in situ* study performed by Schafer *et al*[22] failed to detect Cu_2O during the growth of HKUST-1 via anodic dissolution suggests that further study is needed.

Conclusions

ec-AFM has been used for the first time to monitor the *in situ* growth of a MOF coating using anodic dissolution. Using the archetypal MOF HKUST-1 as a test study, real time electrode observations have supported many previously proposed mechanistic steps for the anodic dissolution coating growth, including the necessity of a "critical concentration" in order to

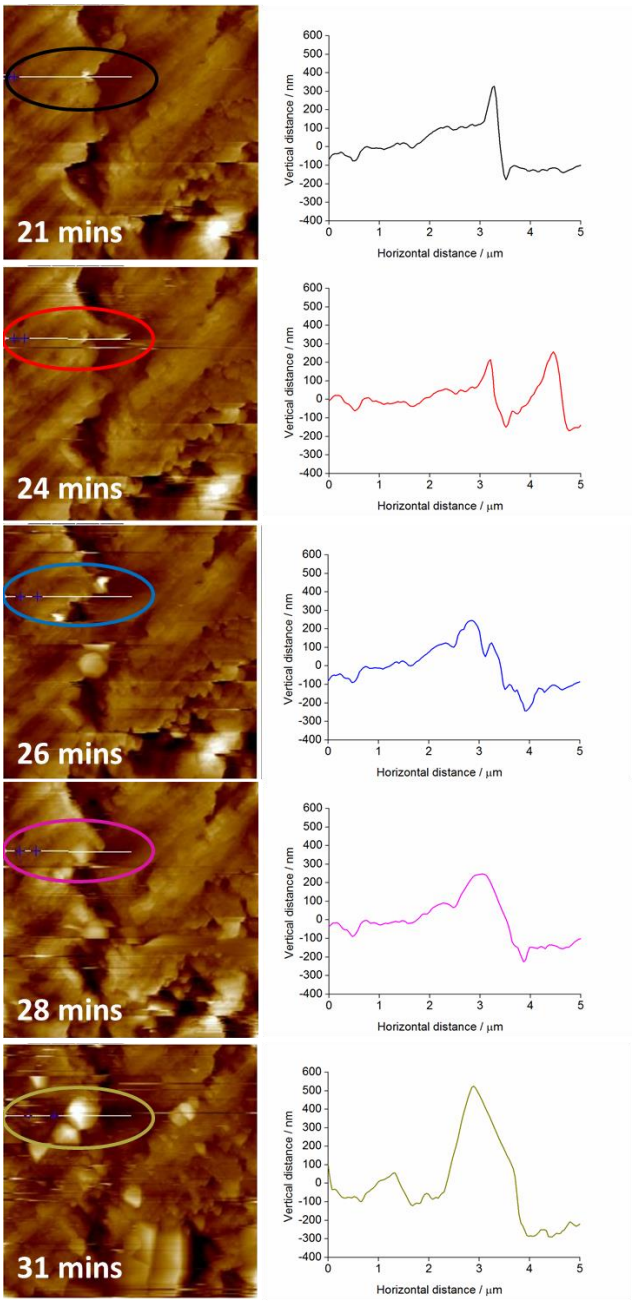

Fig. 5 Height AFM images, 10 x 10 μm, taken during electrochemical growth of a HKUST-1 coating with cross sections (left) plotted (right) to show growth of a HKUST-1 crystal.

initiate growth, nucleation occurring at defects in the roughened electrode surface, and of the early stages of coating growth proceeding via an "island growth" mechanism. Conversely doubt has been cast, with supporting data from *in situ* electrochemical Raman spectroscopy measurements, on the role and indeed even the presence of Cu_2O as an intermediate in the formation of the HKUST-1 coating in the presence of water, as has also been noted previously at lower water concentrations than that used in this work.[22]

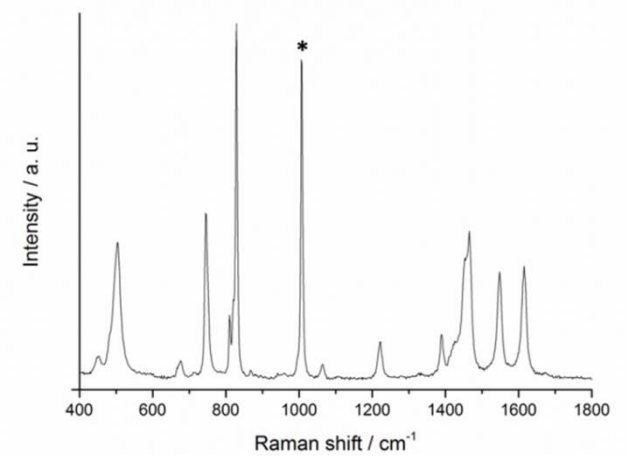

Fig. 6 Raman spectra of HKUST-1. Peak marked with an * used for monitoring HKUST-1 growth at the electrode surface during *in situ* Raman spectroscopy.

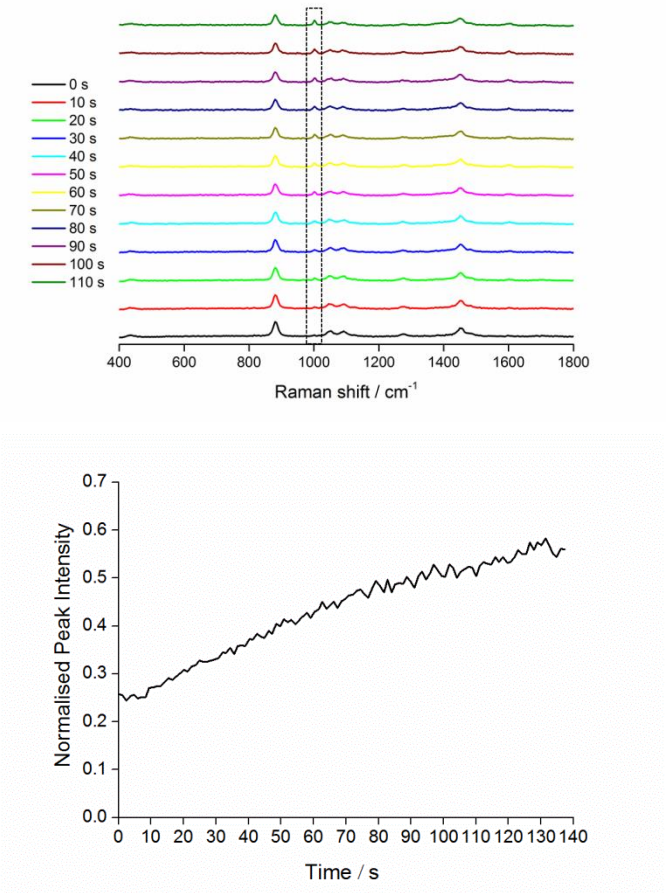

Fig. 7 Raman spectra of the anode surface taken every 1s during the first 2 minutes of the electrochemical growth of a HKUST-1 coating in 3:1 ethanol:H_2O with the growth of the peak at 1000 cm^{-1} highlighted (top) and the variation in the peak intensity of HKUST-1 at 1000 cm^{-1}, normalised to a solvent peak at 2930 cm^{-1}, versus time.

Conflicts of interest

There are no conflicts to declare.

Acknowledgements

SDW would like to thank Dr Hollie Patten, Dr Deborah Lomax and Shiyu Xu for advice and training on the use of and data analysis from the *in situ* ec-AFM set up. SDW would like to thank the NoWNANO DTC and EPSRC for funding.

References

1. G. Ferey, *Chem. Soc. Rev.*, 2008, **37**, 191-214.
2. S. D. Worrall, M. A. Bissett, P. I. Hill, A. P. Rooney, S. J. Haigh, M. P. Attfield and R. A. W. Dryfe, *Electrochim. Acta*, 2016, **222**, 361-369.
3. S. Han, Y. Wei, C. Valente, I. Lagzi, J. J. Gassensmith, A. Coskun, J. F. Stoddart and B. A. Grzybowski, *J. Am. Chem. Soc.*, 2010, **132**, 16358-16361.
4. R. Banerjee, A. Phan, B. Wang, C. Knobler, H. Furukawa, M. O'Keeffe and O. M. Yaghi, *Science*, 2008, **319**, 939-943.
5. N. Campagnol, E. R. Souza, D. E. De Vos, K. Binnemans and J. Fransaer, *Chem. Commun.*, 2014, **50**, 12545-12547.
6. S. D. Worrall, H. Mann, A. Rogers, M. A. Bissett, M. P. Attfield and R. A. W. Dryfe, *Electrochim. Acta*, 2016, **197**, 228-240.
7. S. D. Worrall, M. A. Bissett, W. Hirunpinyopas, M. P. Attfield and R. A. W. Dryfe, *J. Mater. Chem. C*, 2016, **4**, 8687-8695.
8. P. Horcajada, C. Serre, D. Grosso, C. Boissière, S. Perruchas, C. Sanchez and G. Férey, *Adv. Mater.*, 2009, **21**, 1931-1935.
9. I. Stassen, N. Campagnol, J. Fransaer, P. Vereecken, D. De Vos and R. Ameloot, *CrystEngComm*, 2013, **15**, 9308-9311.
10. Y. Mao, L. Shi, H. Huang, W. Cao, J. Li, L. Sun, X. Jin and X. Peng, *Chem. Commun.*, 2013, **49**, 5666-5668.
11. S. Hermes, F. Schröder, R. Chelmowski, C. Wöll and R. A. Fischer, *J. Am. Chem. Soc.*, 2005, **127**, 13744-13745.
12. D. Witters, S. Vermeir, R. Puers, B. F. Sels, D. E. De Vos, J. Lammertyn and R. Ameloot, *Chem. Mater.*, 2013, **25**, 1021-1023.
13. C. M. Doherty, G. Grenci, R. Riccò, J. I. Mardel, J. Reboul, S. Furukawa, S. Kitagawa, A. J. Hill and P. Falcaro, *Adv. Mater.*, 2013, **25**, 4701-4705.
14. C. Carbonell, I. Imaz and D. Maspoch, *J. Am. Chem. Soc.*, 2011, **133**, 2144-2147.
15. I. Hod, W. Bury, D. M. Karlin, P. Deria, C.-W. Kung, M. J. Katz, M. So, B. Klahr, D. Jin, Y.-W. Chung, T. W. Odom, O. K. Farha and J. T. Hupp, *Adv. Mater.*, 2014, **26**, 6295-6300.
16. M. Li and M. Dincă, *J. Am. Chem. Soc.*, 2011, **133**, 12926-12929.
17. R. Ameloot, L. Stappers, J. Fransaer, L. Alaerts, B. F. Sels and D. E. De Vos, *Chem. Mater.*, 2009, **21**, 2580-2582.
18. U. Muller, H.Putter, M. Hesse, M.Schubert, H. Wessel, J. Huff and M. Guzmann, US Pat, 20070227898A1, 2004, BASF SE.
19. N. Campagnol, T. R. C. Van Assche, M. Li, L. Stappers, M. Dinca, J. F. M. Denayer, K. Binnemans, D. E. De Vos and J. Fransaer, *J. Mater. Chem. A*, 2016, **4**, 3914-3925.
20. P. Schafer, M. A. van der Veen and K. F. Domke, *Chem. Commun.*, 2016, **52**, 4722-4725.
21. S. S.-Y. Chui, S. M.-F. Lo, J. P. H. Charmant, A. G. Orpen and I. D. Williams, *Science*, 1999, **283**, 1148-1150.

22. P. Schäfer, A. Lalitha, P. Sebastian, S. K. Meena, J. Feliu, M. Sulpizi, M. A. van der Veen and K. F. Domke, *J. Electroanal. Chem.,* 2017, **793**, 226-234.
23. I. Stassen, M. Styles, T. Van Assche, N. Campagnol, J. Fransaer, J. Denayer, J.-C. Tan, P. Falcaro, D. De Vos and R. Ameloot, *Chem. Mater.*, 2015, **27**, 1801-1807.
24. J. H. Cavka, S. Jakobsen, U. Olsbye, N. Guillou, C. Lamberti, S. Bordiga and K. P. Lillerud, *J. Am. Chem. Soc.*, 2008, **130**, 13850-13851.
25. R. Wagia, I. Strashnov, M. W. Anderson and M. P. Attfield, *Cryst. Growth. Des.*, 2018, **18**, 695-700.
26. P. Cubillas, K. Etherington, M. W. Anderson and M. P. Attfield, *CrystEngComm*, 2014, **16**, 9834-9841.
27. P. Cubillas, M. W. Anderson and M. P. Attfield, *Chem. – Eur. J.*, 2013, **19**, 8236-8243.
28. N. S. John, C. Scherb, M. Shoaee, M. W. Anderson, M. P. Attfield and T. Bein, *Chem. Commun.*, 2009, 6294-6296.
29. D. J. Lomax and R. A. W. Dryfe, *J. Electroanal. Chem.*, 2017.
30. Y. Deng, A. D. Handoko, Y. Du, S. Xi and B. S. Yeo, *ACS Catal.*, 2016, **6**, 2473-2481.